Journal of The Electrochemical Society, **152** (5) A937-A946 (2005)
0013-4651/2005/152(5)/A937/10/$7.00 © The Electrochemical Society, Inc.

Impact of 2-Vinylpyridine as Electrolyte Additive on Surface and Electrochemistry of Graphite for C/$LiMn_2O_4$ Li-Ion Cells

S. Komaba,[a,*,c,z] T. Itabashi,[a] T. Ohtsuka,[a] H. Groult,[b,*] N. Kumagai,[a,*] B. Kaplan,[a,b] and H. Yashiro[a,*]

[a]*Department of Frontier Materials and Functional Engineering, Graduate School of Engineering, Iwate University, Iwate 020-8551, Japan*
[b]*Pierre and Marie Curie University, CNRS UMR 7612, 75252 Paris Cedex 05, France*

For lithium-ion batteries of C/(spinel Li-Mn-O), severe capacity loss occurs after storage of the battery at >50°C. According to our previous studies, this occurrence is predominantly attributable to degradation of the carbon anode, which was induced by electroreduction of Mn(II) dissolved from the spinel; this step is followed by the irreversible electrochemical reaction at the graphite/(Mn deposits)/electrolyte interface. 2-Vinylpyridine (VP) used as an additive in the electrolyte suppressed this degradation; therefore, improving the battery performances. During the first "charge," the electrochemical reductive polymerization of VP monomers at about 0.9 V *vs.* Li/Li^+ resulted in the film formation of poly(2-vinylpyridine) on the graphite surface. The quantity of charge passed for the polymeric film formation depends on the amount of VP addition. Surface analyses using X-ray photoelectron spectroscopy and electron microscopy confirmed that the electrodeposited film blocked the electroreduction of dissolved Mn(II) on the graphite electrode.
 [DOI: 10.1149/1.1885385]

Manuscript submitted September 28, 2004; revised manuscript received December 2, 2004.
Available electronically March 30, 2005.

Among the candidates for the cathode materials of rechargeable Li(-ion) batteries, manganese oxides are attractive due to the low cost of the raw materials and the fact that manganese is considered more environmentally friendly than other transition-metal oxide systems, such as $LiCoO_2$, $LiNiO_2$, and their derivatives. So far, the preparation and characterization of manganese-based oxides have been studied, such as the spinel $LiMn_2O_4$,[1-4] MnO_2s,[5] layered $LiMnO_2$s,[6,7] and $LiNi_{1/2}Mn_{1/2}O_2$.[8,9] In recent years, most research is focusing on the improvement of the battery performance of the spinel $LiMn_2O_4$ and $LiNi_{1/2}Mn_{1/2}O_2$ phases. Among these manganese-based oxides, the spinel-type $LiMn_2O_4$ system is one of the most attractive cathodes in terms of cyclability, operation potential, cost, abundance, and low toxicity. However, a serious problem hindering the wider use of the spinel as the cathode is its poor storage performance at >50°C due to the manganese dissolution. Several mechanisms for the Mn dissolution and its suppression methods have been addressed by some groups.[4,10-14] We recently emphasized that the carbon anode deteriorated after the manganese dissolution into the electrolyte of the carbon/$LiMn_2O_4$ system.[15,16] After the manganese dissolution from the spinel $LiMn_2O_4$ cathode at the higher temperature, the soluble manganese ingredient reaches the carbon anode through the separator, and then the ionic manganese, Mn(II), is readily reduced on the carbon because the standard redox potential of Mn/Mn(II) (*ca.* 1.8 V *vs.* Li/Li^+) is much higher than that of the lithium intercalation into graphite (*ca.* 0.3-0 V *vs.* Li/Li^+).[16,17] We concluded that the higher temperature degradation (>50°C) of the carbon/$LiMn_2O_4$ system was mainly caused by the degradation on the anode side. Therefore, we believe that solving the problem of this anode deterioration is very important for the enhancement of the entire carbon/$LiMn_2O_4$ system, which is applicable to hybrid and pure electric vehicles. Recently, as electric bikes (*i.e.*, electrically assisted bicycles) equipped with lithium-ion batteries of the low cost C/$LiMn_2O_4$ system have been commercialized by some companies, both the bike and C/$LiMn_2O_4$ are gradually becoming more popular.

On the spinel-type $LiMn_2O_4$ cathode side, Xia *et al.* found that both the charge-discharge profile and the structural changes are closely related to the degree of oxygen deficiency created in the synthesis process. Furthermore, their effects on the capacity fading are much more important than the Li/Mn ratio or other factors.[2,18,19] Although controlling the stoichiometry of the $LiMn_2O_4$ material and the suppression of Mn(II) dissolution from the spinel are essentially important for enhanced performance, the "dissolved Mn-free" in the high temperature range would still be difficult to solve the degradation problem of the C/(spinel Li-Mn-O) cell to the best of our knowledge. Therefore, in the C/(spinel Li-Mn-O) system, the protection of the negative electrode against soluble Mn(II) in an electrolyte is considered to be important and useful for understanding and improving the battery performance.

However, to improve the negative electrode performance in lithium-based secondary batteries, some organic/inorganic additives are effective depending on the nature of the anode materials: CO_2,[20] HF,[21,22] HI,[23] AlI_3, and MgI_2[24,25] for metallic lithium, and ethylene sulfite,[26] vinylene carbonate (VC),[27-29] chloroethylene carbonate,[30] and sodium ion[31] for carbon anodes. These additives exhibited a significant effect on the solid electrolyte interface (SEI) formation during the first charge (Li intercalation) process and play a key role in determining the battery performance. The SEI layer containing a polymeric material was also studied to improve the battery performance, such as polypyrrole.[32] Electrochemical polymerization is one of the most interesting and simplest techniques for fabricating a polymer-modified electrode.[33,34] It is believed that vinyl-type polymers synthesized by electroreduction[35,36] are advantageous for direct film formation on a negative electrode in lithium-ion cells, as pointed out by Besenhard and Winter's group.[37]

With the aim of suppressing the degradation of the graphite performance due to dissolved Mn(II), we recently evaluated three inorganic additives: LiI, LiBr, and NH_4I.[38] As we recently communicated, coating the graphite surface with an electropolymerized film of 2-vinylpyridine (VP) used as an electrolyte additive effectively inhibited the degradation by dissolved Mn(II), whereas the VC additive hardly eliminated the degradation.[39] In the present study, we report the impact of the VP additive on the electrode surface and the electrochemistry of graphite in C/$LiMn_2O_4$ cells.

Experimental

Reagent grade natural graphite (Nakalai Tesque, Inc., average particle size about 10 μm), manganese(II) perchlorate (Kanto Chemical Co., Inc.), VP, and VC were used. Battery grade lithium foil, ethylene carbonate (EC), diethyl carbonate (DEC), and $LiClO_4$ were used without any further purification. Details of the experimen-

* Electrochemical Society Active Member.
[c] Present address: Department of Applied Chemistry, Faculty of Science, Tokyo University of Science, Tokyo 162-8601, Japan.
[z] E-mail: komaba@iwate-u.ac.jp

tal conditions are described in our previous paper.[16,31] Manganese(II) perchlorate was dried in vacuum at 100°C for >1 day to remove the residual water prior to its use in the electrochemical cell.

The natural graphite powder was heat-treated at 700°C for 12 h under an Ar atmosphere, and then the working electrodes were prepared by blending the graphite (about 12 mg) and poly(vinylidene fluoride) (9:1 in weight) in *N*-methyl pyrrolidone. The obtained slurry was pasted on a Ni mesh, and dried at 100°C for 24 h. The pressed electrode was dried again at 100°C for 4 days. Li foils were used for both the reference and counter electrodes. The electrolyte was 1 mol dm^{-3} $LiClO_4$ in EC/DEC (1:1 by volume). VP (1, 0.5, and 0.1% by volume) or 6.6 vol % VC as the electrolyte additive was dissolved in the electrolyte solution before the electrochemical cell assembly. The volume of the electrolyte solution in the working electrode compartment of the electrochemical cell was approximately 14 cm^3.[16]

The "charge" (lithium intercalation) and "discharge" (lithium deintercalation) tests at a constant current of 35 mA g^{-1} were carried out between 0.02 and 1.5 V *vs.* Li/Li^+ at room temperature (25 ± 2°C) in a glove box under an argon atmosphere whose dew point was less than −80°C (corresponding to 0.53 ppm by volume of water content). Cyclic voltammetry was performed at a slow sweep rate of 0.05 mV s^{-1} between 1.0 and 0.02 V. To examine the influence of an additive on the degradation of the graphite electrode by soluble Mn(II), a specific amount of a concentrated manganese(II) perchlorate EC/DEC solution was added to the electrolyte solution of a cell to adjust the concentration of 150 ppm Mn(II) when the fifth "discharge" was finished, and then the charge-discharge cycle was started again from the sixth cycle.[16] Alternating current impedance measurements were performed in the frequency range from 100 kHz to 10 mHz with a perturbation voltage of 10 mV.

The surface morphologies of the electrodes were observed using a scanning electron microscope (SEM, Hitachi N-2300NII) equipped with an energy dispersive X-ray analysis (EDX) microanalyzer. X-ray photoelectron spectroscopy (XPS, Perkin Elmer, PHI 5600 system) was employed using monochromatic Al Kα as the incident X-rays, and depth profiling was made by argon ion-beam sputtering which was conducted using an ion-beam voltage of 3 kV. Calibration of the peak position was made by the peak at 284.4 eV corresponding to the C in the hydrocarbon adsorbed on samples; this was used as a reference for the final adjustment of the energy scale. Prior to the SEM or XPS measurement, the electrode after an electrochemical test was rinsed in a pure DEC solution and dried in vacuum, and then transferred to the observation chamber using a specially built transport bag to prevent any exposure to air.

The UV-visible absorption spectra were measured for methanol solutions containing the deposited polymer because the electrodeposited poly(2-vinylpyridine) is partly soluble in methanol.[36] After the first cycle, the graphite electrodes were washed with pure DEC and dried under vacuum, and then the dried electrode was soaked in a specific amount of methanol for one day. The UV-vis absorption of the obtained methanol solution was measured in air.

Results and Discussion

Influence of VP addition on graphite electrode performance.—We first investigated the influence of the VP addition to the electrolyte on the electrochemical performance of a graphite electrode. Figure 1 shows the initial charge-discharge curves of graphite electrodes in electrolyte solutions containing various concentrations of VP. In the VP-free electrolyte, the graphite electrode exhibited a reversible capacity of 328 mAh g^{-1} with typical plateaus corresponding to the Li intercalation stages, and an irreversible capacity of 71 mAh g^{-1} was observed on the first cycle, which is well known to be due to the electroreductive decomposition of the electrolyte components including the SEI formation on graphite around 0.8-0.3 V. In the VP-added electrolytes, an additional plateau clearly appeared around 0.9-1.0 V in the curves earlier than the electroreductive decomposition.

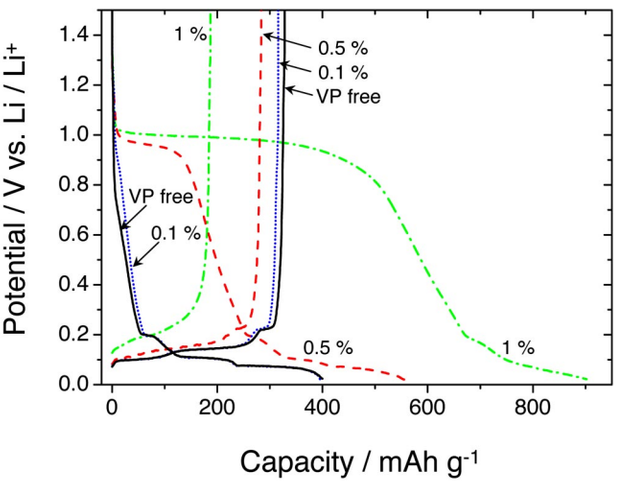

Figure 1. Galvanostatic charge-discharge curves during the first cycle of graphite electrodes at 35 mA g^{-1} in 1 mol dm^{-3} $LiClO_4$ EC/DEC (1:1) with 1, 0.5, 0.1 vol % VP and no VP.

It is thought that this is due to the polymerization induced by the electrochemical reduction of VP monomers as depicted in Scheme 1 based on the previous literature,[35,36] thus resulting

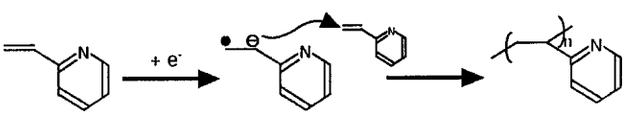

Scheme 1.

in the formation of poly(2-vinylpyridine)[39]

This electroreductive polymerization produces a polymer coating on the graphite during the initial "charge" because the polymer would be insoluble in the electrolyte. The quantity of the reductive charge passed at the plateau increased with increasing VP concentration from 0.1 to 1 vol %. Probably the amount of deposited polymer also increased for the higher VP concentration. For higher amounts of the additive, the potential plateau between 0.20-0.02 V for lithium intercalation into graphite decreased; that is, the thicker polymer film covering the electrode interferred with the lithium intercalation into graphite. A similar tendency was observed for the deintercalation process of lithium from graphite; that is, the initial "discharge" capacities decreased as the concentration of VP became higher. Furthermore, no plateaus were observed between 0.3 and 1.5 V in the discharge curves at all though the current due to the lithium deintercalation was observed in all the discharge curves. This confirms that the electroreductive polymerization that occurs at *ca.* 1.0 V is not reversible, and the electrode surface was modified by the reduction of VP.

Compared to our previous investigation,[39] the dependence of the VP concentration on the electrochemical results of graphite seems to be different from that of Fig. 1. The electrochemical results for the VP additive were influenced by the surface conditions of the graphite and the amounts of graphite loaded in an electrode. Because graphite was not heat-treated in the work of Ref. 39 while the graphite in this study was pretreated at 700°C as mentioned, the surface condition was different. The specific capacities (*i.e.*, mAh $(g\ of\ graphite)^{-1}$) due to the VP electropolymerization were dependent on the loaded active mass even if the amount (concentration) of the VP additive was the same, because the capacities were calculated on the basis of the graphite load. However, we confirmed that

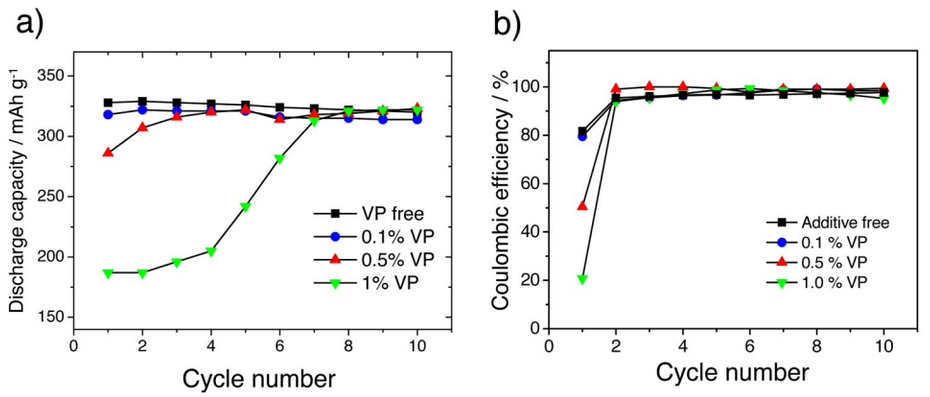

Figure 2. Variations in (a) "discharge" capacity and (b) coulombic efficiency of graphite electrodes at 35 mA g^{-1} in 1 mol dm^{-3} $LiClO_4$ EC/DEC (1:1) with 1, 0.5, 0.1% VP additive and no VP.

the tendency of the dependence on the VP concentration was reproducible under the condition as mentioned in the preceding section.

Figure 2 shows the variations in the "discharge" capacity and coulombic efficiency (defined as "discharge"/"charge" capacity ratio for each cycle) of the graphite electrode in different VP concentrations. In the additive-free electrolyte, the graphite electrode exhibited a high discharge capacity of 328 mAh g^{-1} and the efficiency was relatively high (~100%) except for the first cycle that agrees with the reductive decomposition including the SEI formation. With the addition of VP, the initial discharge capacity and efficiency were monotonously reduced due to the irreversible film formation. For the lower concentration of 0.1% VP, the variations in the "discharge" capacity and efficiency are not significantly different from those of the VP-free one. It is likely that the influence of 0.1% VP is negligible due to the lower amount of the polymer deposit. When the electrolyte contained a higher VP concentration, a reduced capacity and lower efficiency were obtained. Although the polymerization plateau of VP was clearly observed at 0.9 V in the first cycle, the plateau was not distinguishable at all in the subsequent charging, and the efficiency was almost 100% except for the first cycle. Therefore, it was thought that almost all the monomers were consumed in the first cycle; otherwise, the thick polymer film would hinder subsequent electrochemical film formation at the surface. However, during successive cyclings, the "discharge" capacity recovered to show a "discharge" capacity similar to that of the additive-free one, that is, after four and eight cycles for 0.5 and 1%, respectively. We believe that this was due to some crack and/or partial exfoliation in the deposited film which might be promoted by electrochemical cyclings, resulting in the formation of a pathway for the lithium ions.

We also performed cyclic voltammetry to investigate the influence of the VP additive as shown by the cyclic voltammograms (CVs) in Fig. 3. When a larger amount of VP was dissolved in the electrolytes, the reductive peak around 0.9 V *vs.* Li/Li^+ became more preeminent. The limiting reductive current between 0.8 and 0.3 V also increased with the increase in the VP concentration due to the diffusion control of the VP monomers or electric resistance control of the deposited film.[33] The electrochemical polymerization occurred at a higher potential than that of the typical SEI formation of 0.8 V; that is, the polymer was deposited before the SEI formation. It is reasonable to think that the surface film formed in the VP-added electrolytes should differ from the typical SEI film, which allows Li^+ ion transfer and prevents electron transfer, but does not prevent Mn(II) deposition.[16] In other words, the surface film of VP is expected to possess a unique functionality, such as the suppression of the Mn(II) degradation.[39] In Fig. 3, the redox couples below 0.3 V correspond to the reversible lithium intercalation into graphite accompanied by the staging structure. The scan rate of 0.05 mV s^{-1} is relatively fast for separating the redox couples of the staging structures, but it is clear that its electrochemical activity was deteriorated by dissolving a higher concentration of VP, thus resulting in the thicker film formation because of the lower capacity and larger polarization,

Generally, an electropolymerized film on an optically transparent substrate, such as indium-tin oxide-coated glass, readily absorbs UV visible light, and the absorbance is in proportion to its thickness, and the wavelength of absorption peak is related to the band transition depending on the π conjugation and so on.[40] It was difficult to obtain UV-visible absorption spectra of a tested graphite electrode, which is not transparent, but the poly(2-vinylpyridine) film electrochemically formed on a steel surface was partly dissolved in methanol.[36] To prove the electrochemical formation of poly(2-vinylpyridine) on graphite, optical absorption was examined after dissolution in methanol. Figure 4 shows the UV-visible absorption spectra of methanol solutions in which the tested electrode was immersed after the first cycle. For the VP monomer, two absorption peaks exist at 233 nm and 277 nm attributed to the π-π^* electron transformation of the vinyl group and the B absorption band of the aromatic π-π^* one of the pyridine group, respectively, and the peak at 261 nm originates from poly(2-vinylpyridine).[36] Therefore, the appearance of absorption peaks at 261 nm confirms the electrochemical formation of poly(2-vinylpyridine), whose chemical formula can be expressed as $(C_7H_7N)_n$, on a graphite electrode in the EC/DEC medium.

As seen in Fig. 4, very broad peaks appear around 233 and 277 nm, suggesting that the vinyl and pyridine groups were contained in the deposit; therefore, some monomer and/or oligomer molecules would be entrapped in the polymer deposit. As previously described,[36,41] some monomer and solvent molecules were similarly

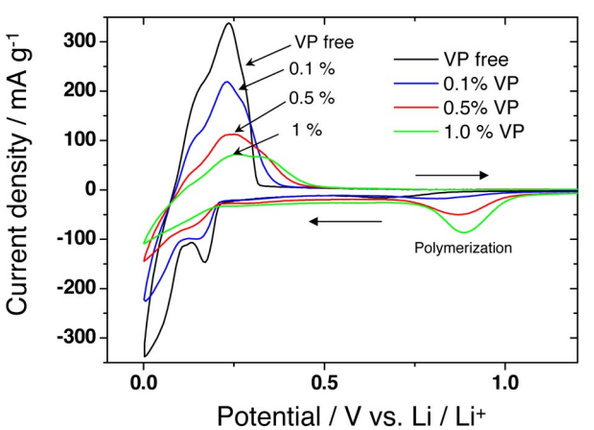

Figure 3. CVs of graphite electrodes at 0.3 mV s^{-1} in 1 mol dm^{-3} $LiClO_4$ EC/DEC (1:1) with 0.1, 0.5, 1% VP additive and no additive.

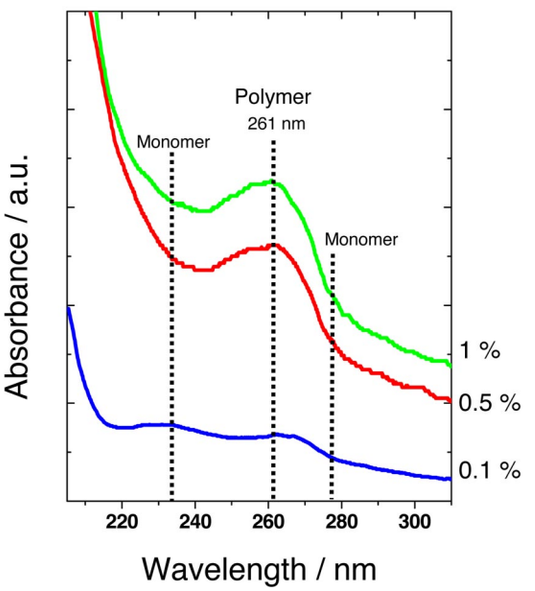

Figure 4. UV-vis absorption spectra of methanol solutions dissolving the electrochemically formed deposits on graphite electrodes with VP additive after the first cycle.

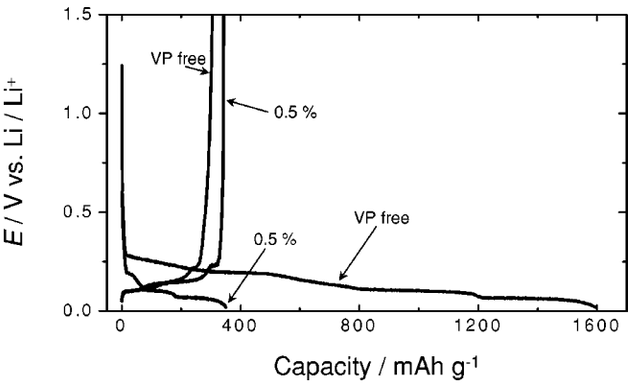

Figure 5. Sixth charge-discharge curves of graphite electrode at 35 mA g^{-1} in 1 mol dm^{-3} $LiClO_4$ EC/DEC (1:1) with 0.5% VP additive and no additive. Manganese(II) perchlorate ([Mn] = 150 ppm) was added before the sixth "charge."

contained in the compact and uniform film, and the film strongly depressed the corrosion of steel. Although the electrode material, solvent, and electrolysis conditions used here were different from those of a previous study, it is postulated that the film formed on graphite possessed a similar chemical nature such as ionic conductivity and reduced electronic conductivity. In consideration of the partial dissolution of the deposited film in methanol, a part of the deposited polymer may be soluble in the organic EC and DEC electrolyte in an electrochemical cell. However, the absorption results demonstrated the formation of a definite amount of the polymer film on the graphite electrode.

Moreover, the entire absorption including the peak situated at 261 nm was intensified by increasing the VP concentration. Although the dissolution of the polymer deposit partly occurred, the higher absorption of the methanol solutions suggested a higher amount of polymer deposition. This agrees with the electrochemical behavior around 0.9 V discussed previously, showing that the graphite surface was covered with the polymer which was thickened by concentrating the VP monomer. The thick polymer interfered with the lithium intercalation into graphite; consequently, we choose the intermediate concentration of 0.5% VP to investigate the influence of the VP coating on the carbon anode degradation by Mn(II). As we describe, this film-forming VP as an electrolyte additive was capable of suppressing the degradation of the graphite anode and, therefore, the improved performances of the graphite/$LiMn_2O_4$ batteries, whereas the addition of VC was hardly effective for the suppression.

Effect of VP addition on suppressing the deterioration by Mn(II).—As previously described,[16,29] when the Mn dissolution occurs in a practical cell after several cycles, the graphite electrode is already modified with the SEI. Therefore, manganese perchlorate [150 ppm Mn(II), where the degradation of battery performance was clearly observed[16]] was dissolved after the fifth "discharge" (before the sixth "charge"), and the charge-discharge cycling behaviors were compared in electrolytes with and without 0.5% VP, as illustrated in Fig. 5. From the sixth curves, the "charge" capacity became significant at *ca.* 1600 mAh g^{-1} with a high irreversibility because the electroreduction of Mn(II) occurred at a higher potential than that of the lithium intercalation followed by the decomposition as previously reported.[16] Also, it seems that there appeared longer plateaus below 0.3 V than those of the lithium intercalation into graphite, because the irreversible reactions simultaneously occurred along with the intercalation in the lower potential range. Surprisingly, the VP addition successfully suppressed these irreversible reactions even though $Mn(ClO_4)_2$ was added to the electrolytes. Furthermore, the potential variation and absolute capacity for the VP-added system were very similar to those obtained in the Mn(II)-free electrolyte. It suggests that the stage structures of the lithium intercalated graphite were successfully formed without any irreversible reactions including the electrochemical plating of Mn metal.

Figure 6 represents the dependence of the "discharge" capacity and coulombic efficiency on the VP addition. For the VP-free

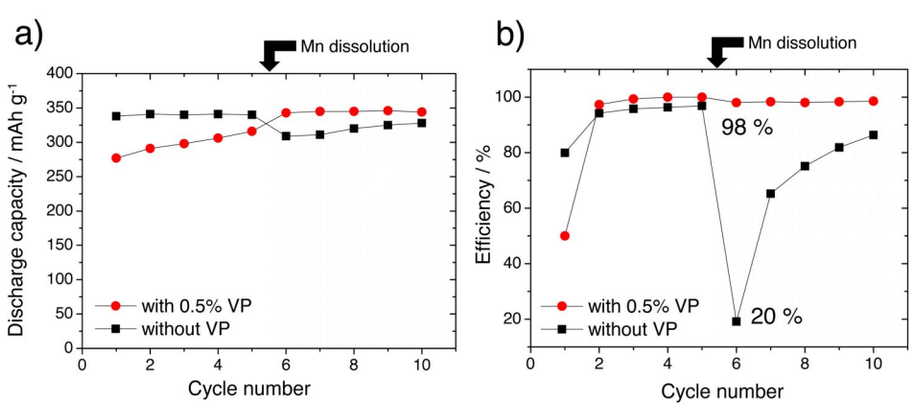

Figure 6. Comparison of (a) "discharge" capacities and (b) coulombic efficiencies of graphite electrodes at 35 mA g^{-1} in 1 mol dm^{-3} $LiClO_4$ EC/DEC (1:1) with 0.5% VP additive and without VP additive. Manganese(II) perchlorate ([Mn] = 150 ppm) was added before the sixth "charge."

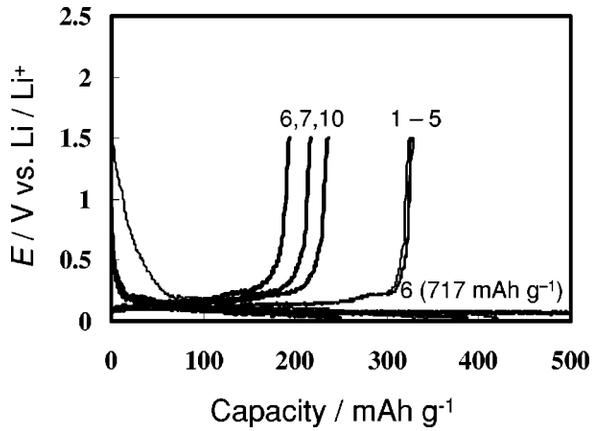

Figure 7. Charge-discharge curves of graphite electrode at 0.1 mA cm^{-2} in 1 mol dm^{-3} $LiClO_4$ EC/DEC (1:1) with 6.6 vol % VC additive. Manganese(II) perchlorate ([Mn] = 150 ppm) was added before the sixth "charge."

sample, the coulombic efficiency at the sixth cycle was dramatically reduced to 20%, which is due to the dissolved Mn(II). Note that this lower efficiency leads to a severe capacity loss in a practical $C/LiMn_2O_4$ cell when considering the absolute capacity (mAh of each electrode) balance of the negative/positive electrodes, even though the capacity recovered in the following cycle between the sixth and tenth cycles as shown in Fig. 6.[16] Therefore, both the discharge capacity and the efficiency of a graphite anode should be simultaneously improved after a 150 ppm Mn(II) addition. During the initial five cycles [without Mn(II) dissolution], the battery performance was hardly affected by the formation of a polymer as mentioned, except for the first cycle that included the polymerization. However, the efficiency at the sixth completely recovered from 20 to 98% with maintenance of the high "discharge" capacity by VP addition. In the cycles subsequent to the fifth, the "discharge" capacity increases ($\sim$340 mAh g^{-1}) with a satisfactory efficiency ($\sim$100%). Additionally, the potential variation and capacities were hardly changed after the Mn(II) addition, as seen in Fig. 5 and 6.

However, the VC additive, which has a polymerizable double bond comparable to VP, positively enhances the performance of the graphite.[27-29] As shown in Fig. 7 and 8, we also examined the charge-discharge test in a VC-added electrolyte for natural graphite as received without heat-treatment at 700°C with the electrochemical conditions the same as in our recent work.[39] When Mn(II) was added to the electrolyte containing VC after the initial five cycles, the "charge" capacity in the VC system reached 717 mAh g^{-1} at the sixth cycle despite the fact that the capacity without VC was 1680 mAh g^{-1}. Furthermore, the "discharge" capacity after the Mn(II) addition decreased to *ca.* 200 mAh g^{-1}, as seen in Fig. 7.

The variations in the "discharge" capacity and coulombic efficiency are represented in Fig. 8. The VC addition made the capacity retention worse between the sixth and tenth cycles, and the efficiency at the sixth one was scarcely improved by the VC addition. It was concluded that VC is hardly capable of depressing the Mn(II) degradation based on these results. There is a general agreement that the SEI film formed on the carbon anode consists of a heterogeneous mixture of inorganic/organic compounds dependent on the electrolyte additives. We believed that the functionality of the surface film formed in the VC system differs from that of the VP; the aromatic pyridine ring should modify the functionality of the surface film to suppress the Mn(II) deposition.

To study the influence of the VP monomers on the electrochemical behavior at the sixth cycle, Fig. 9 compares the CVs for the graphite anode in 150 ppm Mn(II) added electrolytes after the initial five charge-discharge cycles which were performed in Mn(II)-free electrolytes. For both cases, no current peaks are observed between 1.5 and 0.5 V because the SEI formation and/or the electropolymerization were completed before the voltammetry. In the negative scan of Fig. 9, an additional reductive current appeared to be a shoulder between 0.5 and 0.25 V for the VP-free one. Below *ca.* 0.3 V, some redox couples are observed due to lithium de-/intercalation in both CVs; however, the cathodic and anodic currents in the VP-free electrolytes increased and decreased, respectively, showing that an irreversible reaction was induced by the Mn(II) dissolution. From our earlier observation,[16] these phenomena are due to metallic manganese electrodeposition and also the following electrolyte decomposition promoted on the Mn surface. However, the irreversibility was almost completely suppressed by the VP addition; namely, the CV in the VP-added electrolyte confirms that no apparent current flowed above 0.22 V in the cathodic scan, and the redox peaks are identical to that of a typical reversible lithium intercalation accompanied with no side reaction (Fig. 3). These are consistent with the results in Fig. 5 and 6.

When the graphite electrode was "charged" after the Mn(II) addition, the difference in the electrode/electrolyte interface characteristics was investigated by the ac impedance method. Figure 10 shows the Cole-Cole plots obtained at the rest potential in the VP-free and VP-added electrolytes after fully charging to 0.02 V at the sixth cycle. For the locus for the VP-free electrolyte, one semicircle and an inclined line appeared. For the VP addition, two semicircles and an inclined line also appeared. As previously described,[31,42] the first semicircle in the high-frequency region is attributed to the impedance relative to the presence of an SEI layer, and the second in the middle-frequency region is attributed to the charge-transfer process. Finally, the straight line in the low-frequency region is attributed to the Warburg diffusion associated with the finite lithium diffusion in the graphite framework. Apparently, the typical two semicircles and inclined line appeared in the locus for the VP added one. However, one distorted semicircle was observed for the VP-free one. It is likely that understanding the Mn(II) added system may

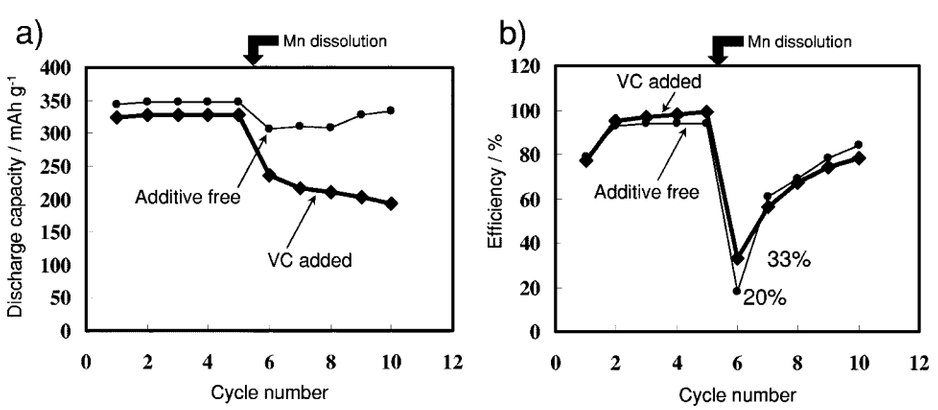

Figure 8. (a) "Discharge" capacities and (b) coulombic efficiencies *vs.* cycle number plots of graphite electrodes at 0.1 mA cm^{-2} in 1 mol dm^{-3} $LiClO_4$ EC/DEC (1:1) with 6.6 vol % VC additive and no additive. Manganese(II) perchlorate ([Mn] = 150 ppm) was added before the sixth "charge."

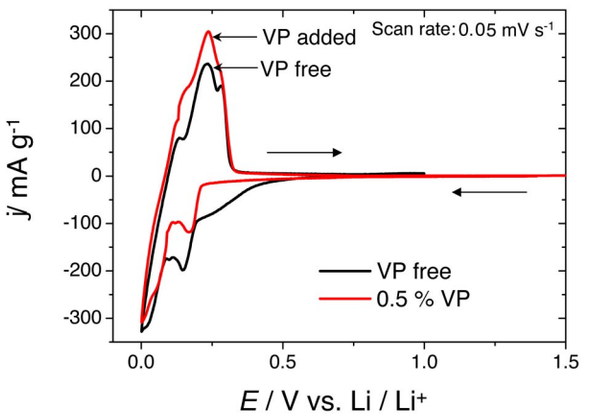

Figure 9. CVs of graphite electrodes after five galvanostatic cycles at 35 mA g^{-1} in 1 mol dm^{-3} $LiClO_4$ EC/DEC (1:1) with/without VP additive. Manganese(II) perchlorate ([Mn] = 150 ppm) was dissolved prior to the voltammetry.

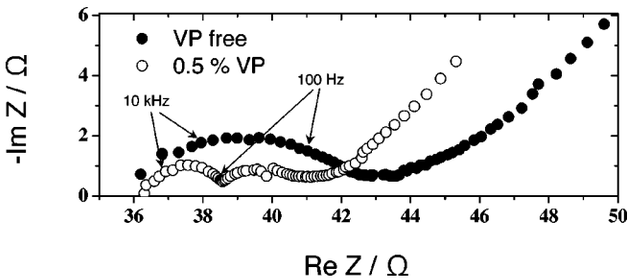

Figure 10. Cole-Cole plots of graphite electrode after sixth "charge" with/without VP additive. Manganese(II) perchlorate ([Mn] = 150 ppm) was added before the sixth "charge."

be complicated because we need to take into account several reactions, such as the Mn(II) reduction, the electrolyte decomposition, and lithium intercalation, resulting in one distorted semicircle which would consist of several semicircles of these reactions having different but close time constants. However, we can safely conclude that the total cell resistance is significantly reduced by the addition of VP in the electrolyte. In the CVs of Fig. 9, the fact that a higher current flowed in the VP-free system seemed to suggest a lower resistance at the interface without VP; however, the reductive current in the CVs included the irreversible deposition of Mn, resulting in a high resistance in the Cole-Cole plots but a higher reductive current in the CVs. Therefore, it was thought that these results from the CVs and the impedance are consistent with each other.

One can conclude that this figure supports the fact that the VP addition suppressed the Mn plating and the induced decomposition, so that the entire impedance and resistances estimated from the semicircles become smaller by the formation of poly(2-vinylpyridine). These electrochemical results confirmed that the VP addition and the formation of a polymer film during the first cycle effectively eliminated the degradation by Mn(II) dissolution. As mentioned here and in previous papers, the electropolymerized film coating protects steels against corrosion,[36] so it is likely that the film formed on graphite protected the lithium intercalated graphite against the Mn(II) ion dissolution. Namely, the protective layer probably possessed a lithium-ion conductivity, but almost no manganese-ion conductivity and almost no electronic conductivity such as the typical SEI layer. Moreover, a stable Mn(II) complex is possibly formed with the pyridine groups of the unreacted monomers, a partly dissolved oligomer or a polymer in an electrolyte solution similar to the Mn(II)-amine complex.[38] Presumably, manganese deposition was also prevented by the complex formation because the stability of the Mn(II) complex would make the reduction of Mn(II) difficult.

Surface analyses of graphite electrode for VP addition.—The VP addition resulted in the formation of a polymer that interferes with the charge transfer between the dissolved Mn(II) and electrode. This fact suggested that the VP addition affected the electrode/electrolyte interface; the condition of the electrode surface after cycling was investigated by SEM, EDX, and XPS as discussed here.

Figure 11 shows SEM images of graphite electrodes cycled in the VP-free and VP added electrolytes to which Mn(II) was added after the initial five cycles. For the VP-free one, graphite particles are not observed at all because an extremely thick deposit covers the graphite electrode on which many small white particles were deposited. It would be formed by the accumulation of metallic Mn and the subsequent significant decomposition products. It is apparent that the degradation of the graphite anode was due to this deposit preventing lithium intercalation into the graphite. Nonetheless, with VP addition, the deposit completely disappeared, and the flake shape of the pristine graphite is still distinguishable even if Mn(II) is added. The surface of the graphite particles is smooth and uniform because there are no small white deposits. As recently reported, some inorganic additives of LiI, LiBr, and NH_4I suppressed the degradation and improved the coulombic efficiency at the sixth cycle when the manganese was dissolved. Compared to these inorganics,[38] the effect of the VP additive is much more remarkable based on the difference in the electrode morphology and cycling behavior. The fact that the deposit did not appear well agrees with the preceding electrochemical results.

From the EDX spectra of the electrode observed by SEM in Fig. 12, chlorine, nickel, and manganese were definitely detected on the surface. Chlorine and nickel come from the perchlorate anion and

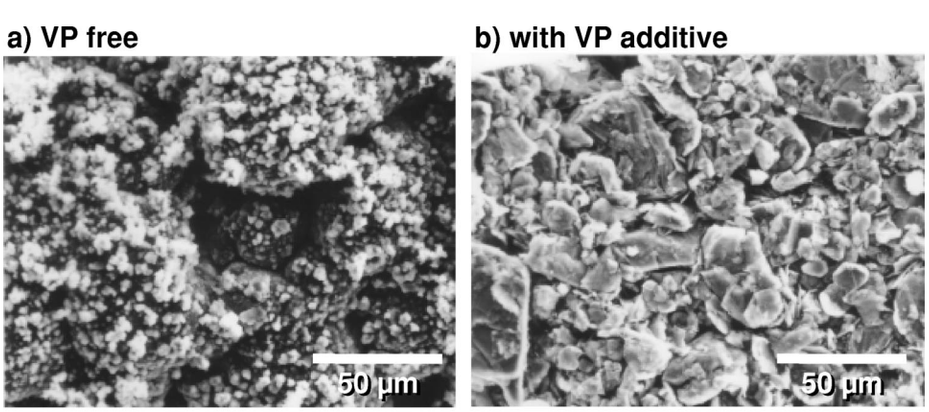

Figure 11. SEM images of graphite electrode (a) without and (b) with VP additive after 10 charge-discharge cycles. Manganese(II) perchlorate ([Mn] = 150 ppm) was added before the sixth "charge."

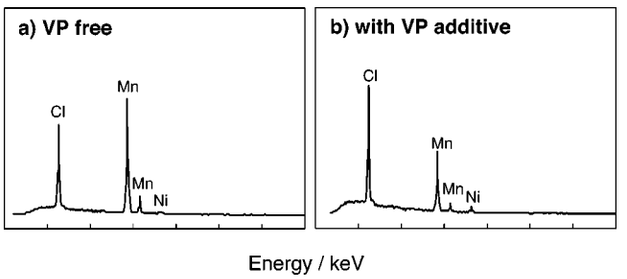

Figure 12. EDX spectra of graphite electrodes cycled (a) without VP and (b) with VP additive after 10 charge-discharge cycles. Manganese(II) perchlorate ([Mn] = 150 ppm) was added before the sixth "charge."

current collector, respectively. Note that the characteristic X-ray intensity of the manganese was weaker for the VP-added electrolyte. This proved that the Mn deposition was suppressed by the film-forming VP additive; namely, the additive depressed the irreversible reactions at the carbon.

Figures 13 and 14 shows the XPS spectra of the Mn 2p, C 1s, O 1s, and N 1s peaks for the electrodes cycled in the VP-added and additive-free electrolytes after dissolving Mn(II) ions. Etching the surface by Ar^+ ion sputtering for 4, 20, and 40 min was carried out to observe the depth distribution. Generally, Ar^+ ion etching of the polymer surface results in surface contamination with the destroyed products; however, the SEI layers and electropolymerized films have already been analyzed by XPS with sputter etching. Because the morphology and thickness based on the SEM analysis (Fig. 11 and 12) were much different between the VP-free and -added systems, the XPS results may contain errors in the surface contamination, but the errors were rather negligible when considering the depth resolution. Under the same etching conditions, the XPS results for both systems were compared for further discussion about the difference in the Mn deposited interface. The relative areas of the Mn 2p, C 1s, O 1s, N 1s, and Li 1s (not shown here) peaks, taking their photoionization cross sections into account, gave the atomic ratios of the important elements as summarized in Table I.

As seen in Fig. 13, Mn $2p_{3/2}$ peaks are clearly observed at the same binding energy for both cases, but with a different thickness and distribution. In the VP addition case, the peaks were remarkably weakened and almost disappeared after sputtering (note that a single peak at *ca.* 640 eV is due to the Auger peak of Ni_{LMM} of the nickel current collector), while the Mn 2p peaks appeared in all the spectra and were intensified by slight etching in the VP-free case (Table I). This proves that the Mn-containing layer became thinner by the electropolymerization of VP. Probably, the existence of Mn with the VP additive was due to adsorption and/or complex formation within a thin solid film of poly(2-vinylpyridine). The voltammetry of a manganese metal electrode in an additive-free electrolyte confirmed its high (electro)chemical reactivity of the electrolyte decomposition;[16,38] therefore, the decomposition products would cover the Mn deposit, so that the peak intensities of Mn for the VP-free electrolyte somewhat increased after sputtering, as seen in Fig. 13 and Table I.

Note that manganese was not metallic (639 eV) and not the dioxide (642 eV), but seemed to be divalent or trivalent such as MnO and Mn_2O_3 as all the Mn $2p_{3/2}$ peaks are situated around 641 eV[39] in Fig. 13. These results suggest the irreversible decomposition and thick deposition by Mn(II) dissolution, as discussed previously. When Mn(II) was dissolved, metallic Mn was first deposited; nevertheless, Mn(II) or Mn(III) compounds, including an organic manganese compound, were readily formed at the surface because of the high reactivity of the Mn metal, as previously described.[16]

From the C 1s spectra, there is also a difference in the chemical state and depth profile of carbon. For the VP-added solution, carbonates (290-289.5 eV) and a hydrocarbon (285 eV)[43] were observed after a 4 min etching; however, an intense peak at 284-285 eV which might be due to carbon in the graphite[44] or a hydrocarbon of the main chain in poly(2-vinylpyridine) appeared after a long sputtering for 20 and 40 min. For the VP-free electrolyte, a peak assigned as C in carbonates is clearly observed during the argon-ion

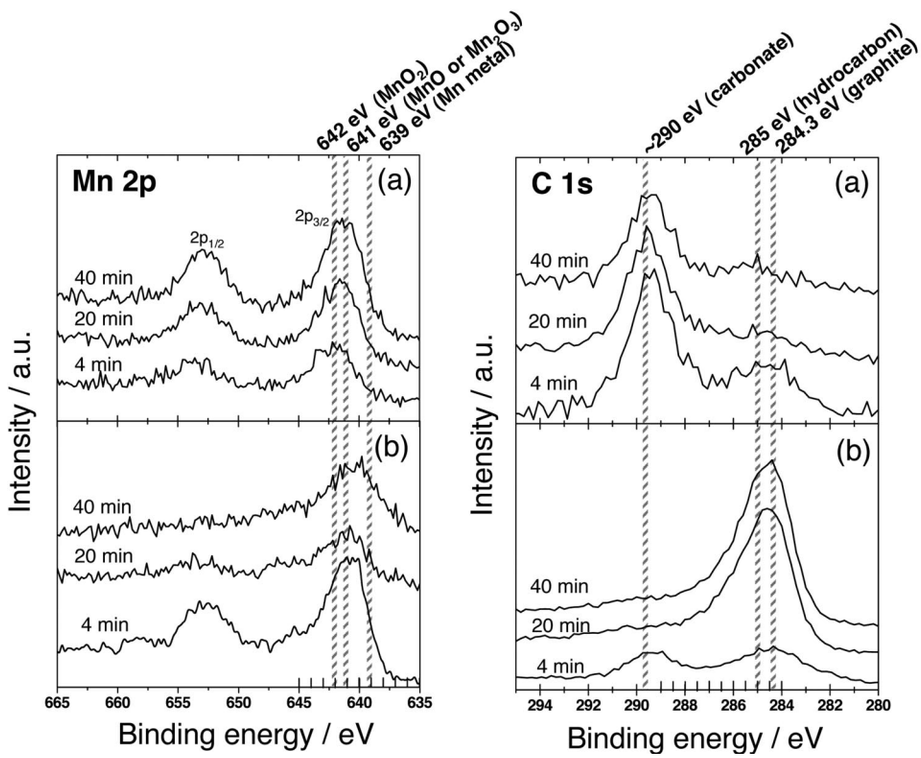

Figure 13. Mn 2p and C 1s XPS narrow spectra of graphite electrodes cycled (a) without and (b) with VP additive after 10 charge-discharge cycles. Manganese(II) perchlorate ([Mn] = 150 ppm) was added before sixth "charge." Times indicate Ar^+ ion etching duration.

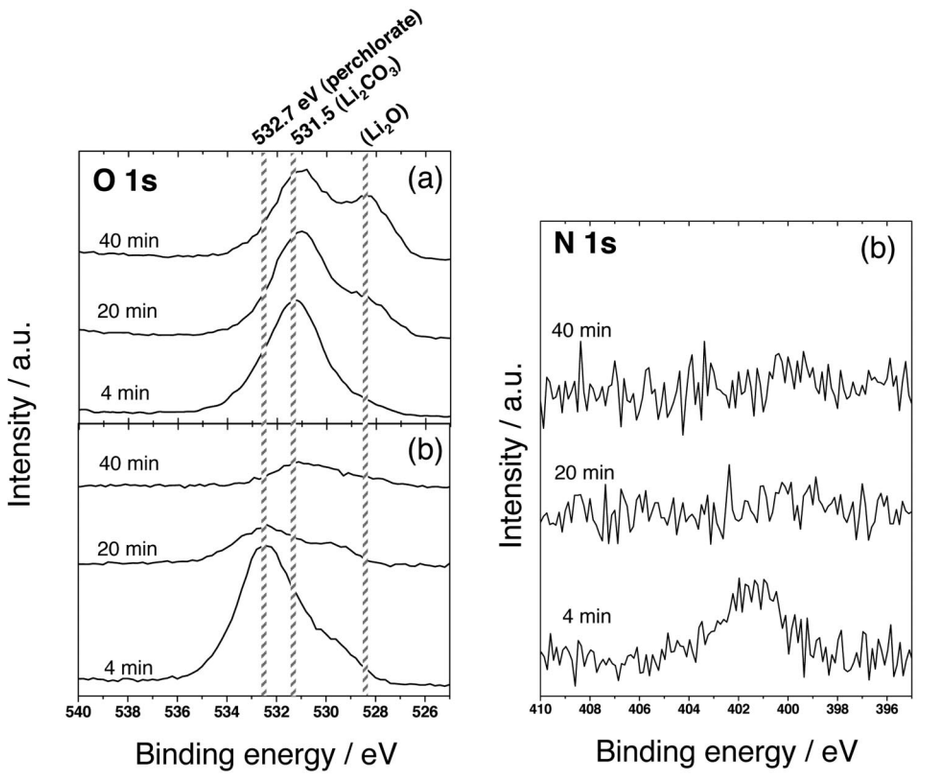

Figure 14. O 1s and N 1s XPS narrow spectra of graphite electrodes cycled (a) without and (b) with VP additive after 10 charge-discharge cycles. Manganese(II) perchlorate ([Mn] = 150 ppm) was added before sixth "charge." Times indicate Ar^+ ion etching duration.

Table I. Atomic ratios (%) of the important elements estimated from the XPS peaks of graphite electrodes with/without VP additive after 10 charge-discharge cycles. Manganese(II) perchlorate ([Mn] = 150 ppm) was added before the sixth "charge."

Sputtering duration (min)	VP free				VP addition				
	C	O	Li	Mn	C	O	N	Li	Mn
4	30.1	50.9	18.7	0.3	42.4	44.5	1.3	9.8	2.0
20	17.4	46.9	32.7	3.0	66.3	16.2	0.6	16.9	[a]
40	13.5	48.4	33.6	4.5	80.5	9.9	0.5	9.1	[a]

[a] Mn 2p peak overlapped the Auger peak of Ni_{LMM} of the Ni current collector, so the estimation of the Mn ratio included a large error.

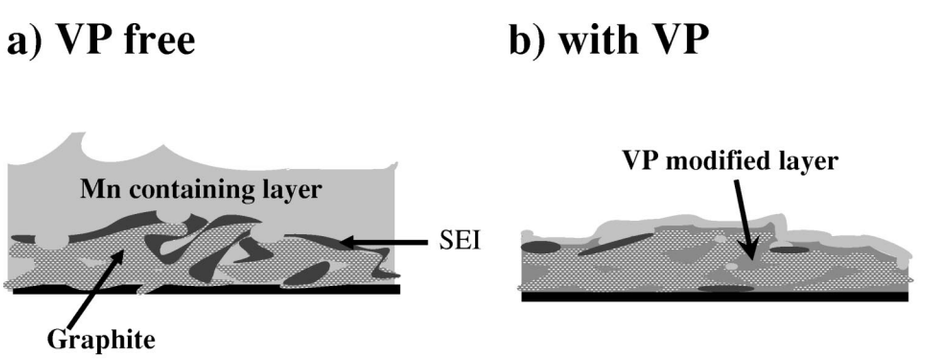

Figure 15. Schematic illustrations of graphite electrode in (a) VP-free and (b) VP added electrolytes after the dissolution of Mn(II) showing that the VP film suppresses the electrochemical deposition of manganese.

etching, and a small hydrocarbon peak was observed; the fact that a peak of C in graphite was not observed is an indication of the presence of a thick layer containing Mn. The carbonates would be attributed to Li_2CO_3 and/or $MnCO_3$. In Fig. 14, the spectrum of N 1s shows the existence of nitrogen which is due to poly(2-vinylpyridine) on the electrode, and the peak attributed to N disappeared after successive etching, indicating that the poly(2-vinylpyridine) film was relatively thin and can protect the graphite surface against dissolved manganese, which agreed with the result in Fig. 11. The O 1s spectra similarly supported the fact that the thick deposit containing a Mn compound was formed in a VP-free electrolyte. That is, peaks assigned as O in Li_2O and carbonates are confirmed after etching. For the VP addition, the peak at 532.7 eV is attributed to oxygen in ClO_4^-,[45] which is probably adsorbed on the polymer surface, but the peaks of oxygen gradually decreased by etching. These XPS results of carbon, oxygen, and nitrogen confirmed that the surface film formed with the VP addition consisted of not only poly(2-vinylpyridine) but also lithium carbonate and a hydrocarbon. It is thought that the VP additive modifies the surface layer.

These surface analyses results are consistent with the formation of thick deposits containing Mn which is attributed to the irreversible electrochemical reduction as mentioned above. Figure 15 shows a schematic model of the surface of a graphite electrode based on the electrochemical and surface analyses. For the VP-free electrolyte, when Mn(II) was dissolved in an electrolyte, Mn metal was first deposited on the electrode, followed by a drastic decomposition of the electrolyte by the metal. Finally, a thick layer containing Mn(II)/(III) compounds interfered with the lithium intercalation. When VP additives were dissolved into the electrolyte, the polymer layer was formed at *ca.* 0.9 V before the typical electrolyte reduction at *ca.* 0.8 V; therefore, the SEI layer was modified with poly(2-vinylpyridine). This modified layer is capable of eliminating the Mn(II) deterioration, because the modified layer successfully blocks the Mn(II) reduction. A further investigation is required to prove how to suppress the charge transfer between Mn(II) and graphite by the poly(2-vinylpyridine) modified layer.

For lithium-ion batteries of C/(spinel Li-Mn-O), severe capacity loss occurs after storage of the battery at $>50°C$, and it is predominantly attributed to the degradation of the carbon anode which was induced by the electroreduction of Mn(II) dissolved from the spinel. This step would be suppressed by the film-forming additive of 2-vinylpyridine, but VC hardly showed such an effect on the suppression of this degradation. Although the VP additive had the problem of increasing the initial irreversible capacity and high polarization, it would be solved by precoating the graphite powder with poly(2-vinylpyridine) by a chemical technique prior to cell assembly. The stability of the VP monomer at the spinel Li-Mn-O electrode should be investigated for designing a practical cell. Consequently, novel types of additives are essentially important and necessary for the suppression of the deterioration, and further analyses and the development of such additives are now in progress to enhance the C/$LiMn_2O_4$ battery system.

Conclusion

Film-forming VP as an electrolyte additive was capable of suppressing the degradation of the graphite anode. Therefore, it improved the performances of graphite/$LiMn_2O_4$ batteries, whereas the addition of VC was not effective in the suppression. The electrochemical reductive polymerization of VP monomers added to an electrolyte solution occurred at the electrode/electrolyte interface during the first "charge," resulting in the poly(2-vinylpyridine) modified-SEI formation on the graphite surface, as confirmed by electrochemical measurements, UV-vis spectroscopy, and XPS measurements. The surface analyses also confirmed that the electrodeposited film effectively suppressed the electroreduction of the dissolved Mn(II) on the graphite electrode, resulting in enhanced performance of the graphite/$LiMn_2O_4$ cells.

Acknowledgments

The authors thank N. Kumagai, A. Ueyama, S. Takahashi, and S. Kozutsumi for their helpful assistance in the experimental work. This study was financially supported by the 2000-2004 program, *Development of Rechargeable Lithium Battery with High Energy/Power Density for Vehicle Power Sources*, of the Industrial Technology Research Grant Program from the New Energy and Industrial Technology Development Organization (NEDO), Japan.

Iwate University assisted in meeting the publication costs of this article.

References

1. T. Ohzuku, M. Kitagawa, and T. Hirai, *J. Electrochem. Soc.*, **137**, 769 (1990).
2. Y. Xia and M. Yoshio, *J. Electrochem. Soc.*, **143**, 825 (1996).
3. D. Song, H. Ikuta, T. Uchida, and M. Wakihara, *Solid State Ionics*, **117**, 151 (1999).
4. S.-T. Myung, S. Komaba, and N. Kumagai, *J. Electrochem. Soc.*, **148**, A482 (2001).
5. S. Komaba, N. Kumagai, and S. Chiba, *Electrochim. Acta*, **46**, 31 (2000).
6. A. R. Armstrong and P. G. Bruce, *Nature (London)*, **381**, 499 (1996).
7. S.-T. Myung, S. Komaba, and N. Kumagai, *J. Electrochem. Soc.*, **149**, A1349 (2002).
8. T. Ohzuku and Y. Makimura, *Chem. Lett.*, **2001**, 744.
9. S.-T. Myung, S. Komaba, and N. Kumagai, *Solid State Ionics*, **170**, 139 (2004).
10. D. H. Jang and S. M. Oh, *J. Electrochem. Soc.*, **144**, 3342 (1997).
11. G. Amatucci, C. N. Schmuts, A. Blyr, C. Sigala, A. S. Gozdz, D. Larcher, and J-M. Tarascon, *J. Power Sources*, **69**, 11 (1997).
12. A. D. Pasquier, A. Blyr, P. Courjal, D. Larcher, G. Amatucci, B. Gerand, and J-M. Tarascon, *J. Electrochem. Soc.*, **146**, 428 (1999).
13. Y. Xia, Y. Zhou, and M. Yoshio, *J. Electrochem. Soc.*, **144**, 2593 (1997).
14. S. Komaba, N. Kumagai, T. Sasaki, and Y. Miki, *Electrochemistry (Tokyo, Jpn.)*, **69**, 784 (2001).
15. N. Kumagai, S. Komaba, Y. Kataoka, and M. Koyanagi, *Chem. Lett.*, **2000**, 1154.
16. S. Komaba, N. Kumagai, and Y. Kataoka, *Electrochim. Acta*, **47**, 1229 (2002).
17. H. Tsunekawa, S. Tanimoto, R. Marubayashi, M. Fujita, K. Kifune, and M. Sano, *J. Electrochem. Soc.*, **149**, A1326 (2002).
18. X. Q. Yang, X. Sun, M. Balasubramanian, J. McBreen, Y. Xia, T. Sakai, and M. Yoshio, *Electrochem. Solid-State Lett.*, **4**, A117 (2001).
19. Y. Xia, T. Sakai, Y. Fujieda, X. Q. Yang, X. Sun, Z. F. Ma, J. McBreen, and M. Yoshio, *J. Electrochem. Soc.*, **148**, A1326 (2001).
20. T. Osaka, T. Momma, T. Tajima, and Y. Matsumoto, *J. Electrochem. Soc.*, **142**, 1057 (1995).
21. S. Shiraishi, K. Kanamura, and Z. Takehara, *J. Electrochem. Soc.*, **146**, 1633 (1999).
22. S. Shiraishi, K. Kanamura, and Z. Takehara, *J. Appl. Electrochem.*, **29**, 867 (1999).
23. S. Shiraishi, K. Kanamura, and Z. Takehara, *J. Appl. Electrochem.*, **25**, 584 (1995).
24. M. Ishikawa, S. Yoshitake, M. Morita, and Y. Matsuda, *J. Electrochem. Soc.*, **141**, L159 (1994).
25. M. Ishikawa, S. Machino, and M. Morita, *J. Power Sources*, **473**, 279 (1999).
26. G. H. Wrodnigg, J. O. Besenhard, and M. Winter, *J. Electrochem. Soc.*, **146**, 470 (1999).
27. Sanyo Co., *Jpn.* Pat. 3,066,126 (1993).
28. C. Jehoulet, P. Biensan, J. M. Bodet, M. Broussley, C. Moteau, and C. Tessier-Lescourret, Abstract 135, p. 153, *The Electrochemical Society and International Society of Electrochemistry Meeting Abstracts*, Vol. 97-2, Paris, France, Aug 31-Sept 5, 1997.
29. X. Zhang, R. Kostecki, T. J. Richardson, J. K. Pugh, and P. N. Ross, Jr., *J. Electrochem. Soc.*, **148**, A1341 (2001).
30. Z. X. Shu, R. S. McMillan, J. J. Murray, and I. J. Davidson, *J. Electrochem. Soc.*, **143**, 2230 (1997).
31. S. Komaba, T. Itabashi, B. Kaplan, H. Groult, and N. Kumagai, *Electrochem. Commun.* **5**, 962 (2003).
32. B. Veeraraghavan, J. Paul, B. Haran, and B. Popov, *J. Power Sources*, **109**, 377 (2002).
33. S. Komaba and T. Osaka, *J. Electroanal. Chem.*, **453**, 19-23 (1998).
34. S. Komaba, K. Fujihana, T. Osaka, S. Aiki, and S. Nakamura, *J. Electrochem. Soc.*, **145**, 1126 (1998).
35. J. W. Breitenbach, O. F. Olaj, and D. Sommer, *Adv. Polym. Sci.*, **9**, 47 (1972).
36. I. Sekine, K. Kohara, T. Sugiyama, and M. Yuasa, *J. Electrochem. Soc.*, **139**, 3090 (1992).
37. K.-C. Moller, H. J. Santner, W. Kern, S. Yamaguchi, J. O. Besenhard, and M. Winter, *J. Power Sources*, **119-121**, 561 (2003).
38. S. Komaba, B. Kaplan, T. Ohtsuka, Y. Kataoka, N. Kumagai, and H. Groult, *J. Power Sources*, **119-121**, 378 (2003).
39. S. Komaba, T. Ohtsuka, B. Kaplan, T. Itabashi, N. Kumagai, and H. Groult, *Chem. Lett.*, **2002**, 1236.
40. T. Osaka, T. Momma, S. Komaba, and H. Kanagawa, *J. Electroanal. Chem.*, **372**, 201 (1994).

41. M. Yuasa, T. Sugiyama, and I. Sekine, *J. Surf. Finish. Soc. Jpn.*, **44**, 230 (1993).
42. A. Funabiki, M. Inaba, Z. Ogumi, S. Yuasa, J. Otsuji, and A. Tasaka, *J. Electrochem. Soc.*, **145**, 172 (1998).
43. K. Kanamura, H. Takezawa, S. Shiraishi, and Z. Takehara, *J. Electrochem. Soc.*, **144**, 1900 (1997).
44. A. M. Anderson, M. Herstedt, A. G. Bishop, and K. Edström, *Electrochim. Acta*, **47**, 1885 (2002).
45. D. Briggs and M. P. Seah, *Practical Surface Analysis*, Vol. 1, 2nd ed., John Wiley & Sons, New York (1993).